THE JOURNAL OF BIOLOGICAL CHEMISTRY
Vol. 274, No. 47, Issue of November 19, pp. 33296–33299, 1999
Printed in U.S.A.

The Cytochrome *c* Oxidase from *Paracoccus denitrificans* Does Not Change the Metal Center Ligation upon Reduction*

(Received for publication, July 27, 1999, and in revised form, September 10, 1999)

Axel Harrenga and Hartmut Michel‡

From the Max-Planck-Institut für Biophysik, Abteilung für molekulare Membranbiologie, Heinrich-Hoffmann-Straße 7, 60528 Frankfurt am Main, Germany

Cytochrome *c* oxidase catalyzes the reduction of oxygen to water. This process is accompanied by the vectorial transport of protons across the mitochondrial or bacterial membrane ("proton pumping"). The mechanism of proton pumping is still a matter of debate. Many proposed mechanisms require structural changes during the reaction cycle of cytochrome *c* oxidase. Therefore, the structure of the cytochrome *c* oxidase was determined in the completely oxidized and in the completely reduced states at a temperature of 100 K. No ligand exchanges or other major structural changes upon reduction of the cytochrome *c* oxidase from *Paracoccus denitrificans* were observed. The three histidine Cu_B ligands are well defined in the oxidized and in the reduced states. These results are hardly compatible with the "histidine cycle" mechanisms formulated previously.

Cytochrome *c* oxidase (EC 1.9.3.1) is the terminal enzyme in the respiratory chains of mitochondria and many aerobic bacteria (see for reviews Refs. 1 and 2). It catalyzes the electron transfer from cytochrome *c* to molecular oxygen and forms water as the product of the reaction. The free energy of this electron transfer reactions is used to generate an electrochemical proton gradient, which drives protons back through the ATP synthases across the membrane, a process that is coupled to the generation of ATP. A total of eight charges is translocated across the membrane per reduced dioxygen. Because the protons needed for water formation and the electrons donated by cytochrome *c* are taken up from opposite sides of the membrane, a pH and an electric field difference are generated. In addition, the cytochrome *c* oxidase translocates ("pumps") up to four protons per oxygen molecule across the membrane, thereby enhancing the yield of energy conservation. Since the discovery that the cytochrome *c* oxidase is a proton pump (3), the molecular mechanism of proton pumping has remained unclear.

Two fundamentally different types of mechanisms are usually discussed: direct mechanisms in which the redox chemistry is associated with small changes occurring very close to the binuclear center, and indirect mechanisms where the coupling is achieved by major conformational changes in the protein. Many research groups favor a directly coupled proton pump mechanism in combination with a gating element because the energy for the proton pumping is generated by oxygen reduction, which takes place in the binuclear center, the characteristic feature of the heme-copper-containing terminal oxidase superfamily (4). Previously proposed gating mechanisms involve protonation and ligand exchanges on heme a_3 (5), between heme a_3 and Cu_B (6), and on Cu_B (the "histidine cycle", Refs. 7 and 8).

The antibody F_v fragment-mediated crystallization of the bacterial cytochrome *c* oxidase from *Paracoccus denitrificans* (9) allowed to determine its structure in two forms, containing either four or two subunits (10;11). Because there was no electron density for the Cu_B ligand His-325 in the oxidized, azide-treated enzyme, Iwata *et al.* (10) adapted the "histidine cycle" on the grounds of possible multiple conformations of this ligand and two different proton access routes, maintaining strict electroneutrality for the redox changes around the binuclear center (12).

In order to test the "histidine cycle" mechanism and other proposed gating mechanisms, the structure of the cytochrome *c* oxidase from *P. denitrificans* was determined at a temperature of 100 K for the azide-free, completely oxidized, and completely reduced states.

MATERIALS AND METHODS

Protein Preparation and Crystallization—The cytochrome *c* oxidase from *P. denitrificans* complexed with the antibody F_v fragment 7E2C50S was isolated according to Kleymann *et al.* (13). A subsequent high performance liquid chromatography gel filtration was performed on a TSK 3000 column (60 cm × 0.7 cm; TosoHaas, Montgomeryville, PA) in the presence of 10 mM Tris/HCl (pH 7.2), 20 mM NaCl, 0.03% dodecyl-β-D-maltoside to remove the excess of the F_v fragment. The cytochrome *c* oxidase-containing fractions were concentrated up to 20–30 mg/ml using Centriprep concentrators (cut-off 50 kDa; Amicon). Co-crystallization of the cytochrome *c* oxidase with the antibody fragment was performed at 14 °C using the sitting drop vapor diffusion technique with a reservoir solution of 400 mM ammonium acetate (pH 8.0), 7% dimethyl sulfoxide (Me_2SO), and 10–14% polyethylene glycol 2000 monomethylether according to Ostermeier *et al.* (9). For recording optical spectra, the crystals were grown on non-siliconized cover slides in order to fix them by adhesion onto the glass surface.

Measurement of Single Crystal Absorbance Spectra—Optical absorbance spectra of crystals fixed onto glass surfaces were recorded with a single crystal microscope-photometer (Zeiss Microscope UEM, Photometer 03) controlled by λ-Scan software package (Zeiss) (14). The crystals on the glass cover slides were mounted in airtight home-built flow cells filled with the mother liquor (220 mM ammonium acetate, 60 mM Tris/HCl, 60 mM NaCl, 7% Me_2SO, 0.03% dodecyl-β-D-maltoside, and 12% polyethylene glycol 2000 monomethylether (pH 8.0)). They were reduced by exchanging the filling of the flow cell with mother liquor plus 2 mM sodium dithionite. A reference spectrum was recorded with mother liquor next to the crystal.

X-ray Data Collection—For x-ray data collection, the crystals were transferred into 220 mM ammonium acetate (pH 8.0), 60 mM Tris/HCl

* This work was supported by the Fonds der Chemischen Industrie, Sonderforschungsbereich 472 of the Deutsche Forschungsgemeinschaft, and the Max-Planck-Gesellschaft. The costs of publication of this article were defrayed in part by the payment of page charges. This article must therefore be hereby marked "*advertisement*" in accordance with 18 U.S.C. Section 1734 solely to indicate this fact.

The atomic coordinates and structure factors (code 1QLE) have been deposited in the Protein Data Bank, Research Collaboratory for Structural Bioinformatics, Rutgers University, New Brunswick, NJ (http://www.rcsb.org/).

‡ To whom correspondence should be addressed. Tel.: 49-69/96769400; Fax.: 49-69/96769423; E-mail: michel@mpibp-frankfurt.mpg.de.

TABLE I
Data collection and refinement statistics

Redox state	Oxidized	Reduced
Data collection and processing		
Unit cell dimensions		
a (Å)	204.7	206.5
b (Å)	204.7	206.5
c (Å)	80.4	81.4
α, β, γ (°)	90, 90, 90	90, 90, 90
Space group	P4	P4
Number of reflections	165,650	120,987
Unique data	64,653	48,955
Resolution (Å)	3	3.3
$I/\sigma(I)$	9.6	10.5
Completeness (%)	95.2	94.1
R_{merge} (%)[a]	11.5	10.5
Refinement		
No. of protein atoms	10,529	10,529
No. of cofactor atoms[b]	123	123
No. of lipid atoms[b]	108	108
R_{cryst} (%)[c]	23.5	23.6
R_{free} (%)[c]	30.1	29.3
rms deviations from ideal geometry[d]		
Bond length (Å)	0.012	0.009
Bond angles (°)	1.6	1.4
Dihedral angles (°)	23.8	23.8
Improper angles (°)	1.5	1.4

[a] $R_{merge} = \Sigma_h \Sigma_i |I_i(h) - <I(h)>| / \Sigma_h \Sigma_i I_i(h)$.
[b] Cofactor atoms include all heme and bound metal atoms; lipid atoms include the atoms of the two bound phosphatidyl choline molecules.
[c] $R_{cryst} = \Sigma_h || F_{obs}| - k |F_{calc}|| / \Sigma_h |F_{obs}|$. The free R-factor (R_{free}) (30) was calculated for a "test" set of reflections (5%), which were not included in atomic refinement.
[d] With respect to Engh and Huber parameters (18). rms, root mean square.

(pH 8.0), 60 mM NaCl, 7% Me_2SO, 0.03% dodecyl-β-D-maltoside, 12% polyethylene glycol 2000 monomethylether, and 25% glycerol as cryo-buffer. The glycerol concentration was raised in 5% steps. The crystals were frozen in liquid propane at liquid nitrogen temperatures. During data collection the crystals were cooled at 100 K using a cryostream (Oxford Cryosystems). In the case of oxidized crystals, 2 mM potassium hexacyanoferrate (III) was added to all buffers. In order to reduce the crystals, sodium dithionite was added to the cryo-buffer to a final concentration of 5 mM. After 10 min of incubation, the completely reduced crystals were frozen as described.

X-ray diffraction data were collected at the high brilliance beamline ID02 (ESRF, Grenoble, France) with a MAR imaging plate detector in frames of 0.7° through a continuous angular range of 90°. All diffraction data were processed and scaled with the programs DENZO/SCALEPACK (15) and TRUNCATE from the CCP4 program suite (16). Data collection is summarized in Table I.

Model Refinement—The two cryo-structures of the cytochrome *c* oxidase (completely oxidized and completely reduced) were refined with CNS 0.3 (17) using the room-temperature structure of the cytochrome *c* oxidase (10) as a starting model. In the early stages slow cool energy minimization protocols were performed, while in the final stages only positional and grouped B-factor refinement were employed. The force constants derived by Engh and Huber (18) were used as geometrical restraints. A bulk solvent correction and an overall anisotropic temperature factor were applied. σ_A-weighted $2F_o - F_c$ and $F_o - F_c$ electron density maps were calculated with CNS 0.3 (17). For the critical parts of the model, simulated annealing omit electron density maps were generated (19). Model building and inspection of the electron density maps were done using O (20). The overall stereochemical quality of the structure was analyzed using PROCHECK (21), WHAT-CHECK (22), and CNS. The refinement and quality of the final models are summarized in Table I.

RESULTS

Single Crystal Absorbance Spectra—Spectral measurements with single crystals of the cytochrome *c* oxidase show that the enzyme is completely oxidized under the crystallization conditions (Fig. 1). After addition of sodium dithionite, a complete reduction is observed immediately (Fig. 1). Carbon monoxide binds after reduction to heme a_3 as expected.

There is no difference between the optical spectra of the oxidized and of the reduced cytochrome *c* oxidase in the crystals and spectra of the same species in solution.

Structure of the Binuclear Center—Simulated annealing omit electron density maps (19) were calculated for the binuclear center in order to reduce the model bias (Fig. 2). The three histidine ligands of Cu_B (His-276, His-325, His-326) can be detected clearly in the completely oxidized and in the completely reduced state. In contrast, in the structure determined at 18 °C of the oxidized, azide-treated enzyme, no electron density for the ligand His-325 had been observed beyond C_β. As observed for the ligands of Cu_B, the ligand of heme a_3, His-411, does not change its conformation upon reduction. The distance between the heme a_3 iron and Cu_B is 5.2 Å in all structures and therefore appears to be independent of the redox state.

The continuous electron density between Cu_B and the heme a_3 iron observed in the two-subunit cytochrome *c* oxidase from *P. denitrificans* (11) is also visible in the oxidized cryo-structure of the entire enzyme presented here. In the structure of the completely reduced cytochrome *c* oxidase, this electron density is missing.

Redox-coupled Conformational Changes in Other Parts of the Protein—At the present resolution, no conformational changes could be detected in the protein moiety. Helix movements or loop rearrangements can be excluded with certainty. The root mean square difference of the C_α-positions of the oxidized and the reduced subunit I is 0.37 Å, and within the range of the expected statistical error. In addition significant conformational changes cannot be observed around the other metal centers (Cu_A, heme a, Mg^{2+}/Mn^{2+} binding site, and the proposed Ca^{2+} binding site (Ref. 11)).

DISCUSSION

The mechanism of coupling between electron transfer and proton pumping in cytochrome *c* oxidases is a subject of intense studies. The missing electron density for the Cu_B ligand His-325 in the oxidized, azide-treated cytochrome *c* oxidase from *P. denitrificans* (10) can be interpreted in two different ways; (*a*) the treatment of the enzyme with azide results in a ligand displacement on Cu_B, or (*b*) the crystals are partially reduced by free electrons and radicals produced by the x-rays during data collection. Both interpretations indicate a possible structural flexibility of this Cu_B ligand. On the basis of possible multiple orientations for the ligand His-325, the "histidine cycle" (7) was adapted by Iwata *et al.* (10). It predicts that one histidine ligand is not a Cu_B ligand anymore in the completely reduced state. This prediction was tested by the use of cryo-crystallography. Care was taken that the x-ray data were collected on defined redox states. At a temperature of 100 K, structural changes following the possible reduction of the oxidized cytochrome *c* oxidase by radicals and free electrons produced by the x-rays can be prevented. As a second advantage, the reduced enzyme does not react with oxygen and therefore the reduced state can be studied easily. Because only very small crystals can be frozen without drastic lost of crystal quality, the effective resolution is slightly lower than that of the non-frozen crystals (10). The quality of the synchrotron beam must be very high to enable data collection. For the measurements using frozen cytochrome *c* oxidase crystals, the availability of the high brilliance beamline at the European Synchrotron Radiation Facility (Grenoble, France) was absolutely necessary.

In order to show that the experimental procedures resulted in the expected redox states and that these are not influenced by the crystal lattice of cytochrome *c* oxidase, optical absorb-

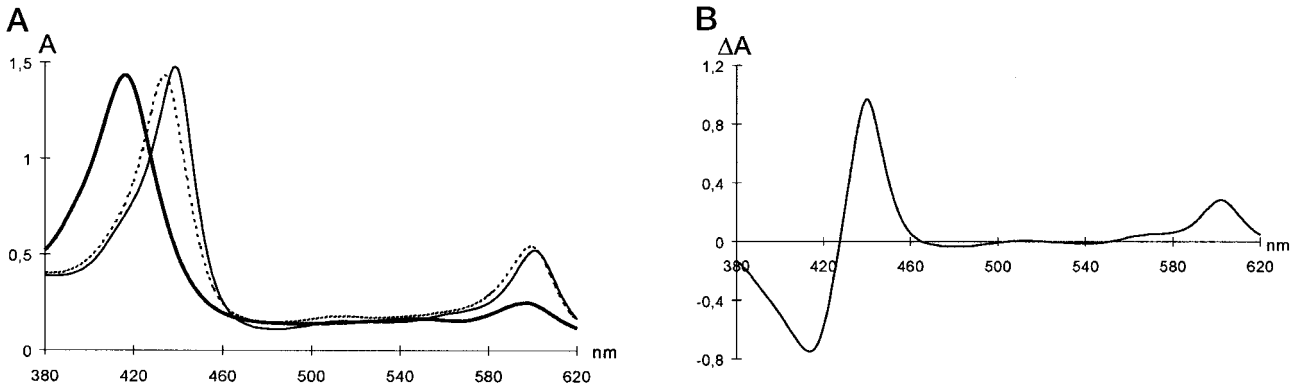

FIG. 1. **Single crystal microspectrophotometry of air oxidized (*thick solid curve*), dithionite reduced (*thin solid curve*), and reduced carbon monoxide-treated (*dashed curve*) cytochrome *c* oxidase crystals from *P. denitrificans*.** *A* shows the absolute spectra and *B* the difference spectra between dithionite reduced and air oxidized crystals.

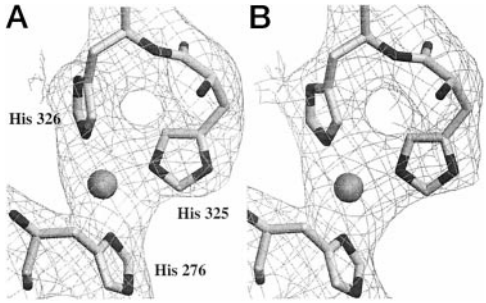

FIG. 2. **Simulated annealing omit electron density maps (19) of Cu_B and the three histidine ligands (counter level 1 σ) for the oxidized cytochrome *c* oxidase measured at 100 K (*A*) and the dithionite reduced cytochrome *c* oxidase measured at 100 K (*B*).** The electron density maps are superimposed on the refined models.

ance spectra were recorded with a single crystal microscope-photometer. The spectra of the cytochrome *c* oxidase crystals do not differ from the spectra of the enzyme in solution. The cytochrome *c* oxidase in the crystals can be reduced and binds carbon monoxide after reduction. It is therefore unlikely that the crystal contacts between adjacent molecules inhibit large domain or helix movements.

One would expect reduction of the metal centers to induce structural changes coupled to proton pumping. However, significant structural differences between the completely oxidized and completely reduced cytochrome *c* oxidase could not be observed at the given resolution. Although high resolution x-ray data could not be collected, the crystallographic measurements show that no ligand exchange occurs at the binuclear center. All three Cu_B ligands are well defined in the completely oxidized and completely reduced states. This observation is in agreement with recent extended X-ray absorption fine structure data, which describe only minor changes at Cu_B of the ubiquinol oxidase from *Escherichia coli* upon reduction (23), whereas the structural changes observed upon ligation with carbon monoxide (23) are hardly compatible with earlier x-ray crystallographic data observed with the bovine heart mitochondrial cytochrome *c* oxidase (24). Additionally, the histidine heme a_3 ligand does not change its conformation in a redox-dependent manner. An exchange with a nearby tyrosine residue has already been ruled out by mutagenesis experiments (25). These results are clearly not compatible with the proposed pumping mechanisms, which postulate ligand exchanges at heme a_3 (5), between heme a_3 and Cu_B (6), and at Cu_B (the "histidine cycle"; Ref. 7).

An indirect mechanism associated with major conformational changes in the protein can also be excluded for this bacterial cytochrome *c* oxidase, because no backbone movements occur in the protein moiety. Such a movement has been described for the bovine heart cytochrome *c* oxidase affecting a loop in subunit I around the residue Asp-51 (24). However, this loop facing the cytoplasm is not conserved in the cytochrome *c* oxidase from *P. denitrificans*. It is only found in cytochrome *c* oxidases of animals. Therefore, it cannot be part of a general mechanism, which must be expected due to the remarkable structural conservation of the key features of this enzyme (10;11;26). Redox structural changes, apart from the movement of this non conserved surface loop, are not described for the bovine heart cytochrome *c* oxidase (24). The most likely explanation for the structural change around Asp-51 observed upon reduction of the bovine cytochrome *c* oxidase is the following; Asp-51 is deprotonated in the oxidized enzyme, and its negative charge is stabilized by the three hydrogen bonds observed with the carboxylate group as acceptor. Upon reduction of Cu_A, which is only 6.7 Å away from this carboxylate group, Asp-51 will be electrostatically repelled from the electron on Cu_A, and assumes its new position further away from Cu_A.

Mechanisms, which involve structural changes of cytochrome *c* oxidases upon reduction, are not compatible with the results of the crystallographic studies, on both the bacterial and the mammalian enzyme. The existence of large volume changes upon reduction postulated on the basis of dilatometry measurements (27) is not observed for the bacterial and mammalian enzymes in the crystallographic studies.

Not only the structure but also the static behavior upon reduction seem to be conserved among the cytochrome *c* oxidases. This feature makes it inevitable that we consider new mechanisms for the coupling between electron transfer and proton pumping which do not involve ligand exchanges or major conformational changes. A new detailed mechanism (28) has been suggested on the basis of the structure and electrostatic calculations (29), proposing that the interplay of the conserved residue Glu-278 with the propionates of the two hemes is sufficient for the proton pumping across the membrane and there is no need for exchanging protonatable metal ligands. In this mechanism protons are taken up from the inner side to balance the charge of the electron. These protons are stored around the heme propionates, and electrostatically repelled and thus pumped by protons approaching the catalytic site in line with Rich's electroneutrality principle (12).

Acknowledgments—We thank J. Behr and A. Kannt for help during data collection and for stimulating discussions, and we are grateful to H. Müller for excellent technical assistance.

REFERENCES

1. Ferguson-Miller, S., and Babcock, G. T. (1996) *Chem. Rev.* **96,** 2889–2907
2. Michel, H., Behr, J., Harrenga, A., and Kannt, A. (1998) *Annu. Rev. Biophys. Biomol. Struct.* **27,** 329–356

3. Wikström, M. K. (1977) *Nature* **266,** 271–273
4. Garcia-Horsman, J. A., Barquera, B., Rumbley, J., Jixiang, M., and Gennis, R. B. (1994) *J. Bacteriol.* **176,** 5587–5600
5. Rousseau, D. L., Ching, Y. C., and Wang, J. (1993) *J. Bioenerg. Biomembr.* **25,** 165–177
6. Woodruff, W. H. (1993) *J. Bioenerg. Biomembr.* **25,** 177–188
7. Wikström, M., Bogachev, A., Finel, M., Morgan, J. E., Puustinen, A., Raitio, M., Verkhovskaja, M., and Verkhovsky, M. I. (1994) *Biochim. Biophys. Acta* **1187,** 106–111
8. Morgan, J. E., Verkhovsky, M. I., and Wikström, M. (1994) *J. Bioenerg. Biomembr.* **26,** 599–608
9. Ostermeier, C., Iwata, S., Ludwig, B., and Michel, H. (1995) *Nat. Struct. Biol.* **2,** 842–846
10. Iwata, S., Ostermeier, C., Ludwig, B., and Michel, H. (1995) *Nature* **376,** 660–669
11. Ostermeier, C., Harrenga, A., Ermler, U., and Michel, H. (1997) *Proc. Natl. Acad. Sci. U. S. A.* **94,** 10547–10553
12. Rich, P. R. (1995) *Aust. J. Plant. Physiol.* **22,** 479–486
13. Kleymann, G., Ostermeier, C., Ludwig, B., Skerra, A., and Michel, H. (1995) *Bio/Technology* **13,** 155–160
14. Fritzsch, G., Buchanan, S., and Michel, H. (1989) *Biochim. Biophys. Acta* **977,** 157–162
15. Otwinowski, Z., and Minor, W. (1997) *Methods Enzymol.* **276,** 307–326
16. Collaborative Computational Project Number 4 (1994) *Acta Crystallogr. Sect. D* **50,** 760–763
17. Brünger, A. T., Adams, P. D., Clore, G. M., DeLano, W. L., Gros, P., Grosse-Kunstleve, R. W., Jiang, J.-S., Kuszewski, J., Nilges, M., Pannu, N. S., Read, R. J., Rice, L. M., Simonson, T., and Warren, G. L. (1998) *Acta Crystallogr. Sect. D* **54,** 905–921
18. Engh, R. A., and Huber, R. (1991) *Acta Crystallogr. Sect. A* **47,** 392–400
19. Hodel, A., Kim, S.-H., and Brünger, A. T. (1992) *Acta Crystallogr. Sect. A* **48,** 851–859
20. Jones, T. A., Zou, J. Y., Cowan, S. W., and Kjeldgaard, M. (1991) *Acta Crystallogr. Sect. A* **7,** 110–119
21. Laskowski, R. A., MacArthur, M. W., Moss, D. S., and Thornton, J. M. (1993) *J. Appl. Crystallogr.* **26,** 283–291
22. Hooft, R. W. W., Vriend, G., Sander, C., and Abola, E. E. (1996) *Nature* **381,** 272
23. Ralle, M., Verkhovskaja, M. L., Morgan, J. E., Verkhovsky, M. I., Wikström, M., and Blackburn, N. J. (1999) *Biochemistry* **38,** 7185–7194
24. Yoshikawa, S., Shinzawa-Itoh, K., Nakashima, R., Yaono, R., Yamashita, E., Inoue, N., Yao, M., Fei, M. J., Libeu, C. P., Mizushima, T., Yamaguchi, H., Tomizaki, T., and Tsukihara, T. (1998) *Science* **280,** 1723–1729
25. Mitchell, D. M., Ädelroth, P., Hosler, J. P., Fetter, J. R., Brzezinski, P., Pressler, M. A., Aasa, R., Malmström, B. G., Alben, J. O., Babcock, G. T., Gennis, R. B., and Ferguson-Miller, S. (1996) *Biochemistry* **35,** 824–828
26. Tsukihara, T., Aoyama, H., Yamashita, E., Tomizaki, T., Yamaguchi, H., Shinzawa-Itoh, K., Nakashima, R., Yaono, R., and Yoshikawa, S. (1996) *Science* **272,** 1136–1125
27. Kornblatt, J. A., Kornblatt, M. J., Rajotte, I., Hoa, G. H. B., and Kahn, P. C. (1998) *Biophys. J.* **75,** 435–444
28. Michel, H. (1998) *Proc. Natl. Acad. Sci. U. S. A.* **95,** 12819–12824
29. Kannt, A., Lancaster, C. R. D., and Michel, H. (1998) *Biophys. J.* **74,** 708–721
30. Brünger, A. T. (1992) *Nature* **355,** 472–474